SSC23-II-08

A Small Satellite Constellation for Monitoring of the Aurora

Giada Staniscia, Bastiaan Lagaune, Sten Berge, Milan Battelino
OHB Sweden, Viderögatan 6, 164 40 Kista, Sweden; +46 726 018 823
giada.staniscia@ohb-sweden.se

Stefan Kraft
ESOC - European Space Agency, Robert-Bosch-Strasse 5, 64293 Darmstadt, Germany

ABSTRACT

As part of the European Space Agency's D3S (Distributed Space Weather Sensor System), a small satellite constellation is currently being designed by OHB Sweden which will observe space weather impacts in Earth's vicinity by monitoring of the auroral oval. The primary objective of the Aurora mission is to observe the Aurora Borealis and Australis continuously and as complete as possible. The auroral emissions are the result of interactions of the Solar Wind and Coronal Mass Ejections with the Earth which drive the location and strength of electron precipitation on the ionosphere. Such observations will thereby allow the identification, characterization and nowcasting of geomagnetic storms and sub-storms. Observation of the auroral emissions is expected to enable improved and new services relevant for critical infrastructures such as communication, satellite navigation, satellite operation, aviation, transport, power network operation, and resource utilization. The core instruments of the Aurora mission are the optical and far UV wide-field imagers. Furthermore, a radiation monitor and a magnetometer are baselined as a secondary payload to monitor magnetic field dynamics and the radiation environment. The availability of additional resources for other payloads relevant for D3S is under investigation. To minimize the number of satellites, while ensuring continuous and guaranteed coverage of the auroral oval, a constellation of four satellites in MEO orbit is envisaged. Such orbit however poses significant challenges for small satellites in terms of accessibility, sustainability, and radiation dose. The heritage microsatellite platform from OHB Sweden, InnoSat (designed for LEO), will thus undergo several upgrades in terms of maneuverability, shielding, communication, and reliability. Of particular importance is the low latency requirement which may favor an Inter-Satellite Link. In a first step ESA is implementing a demonstrator mission that shall be launched in 2027 with the aim of optimizing the performance and preparing the operational satellite constellation considered for implementation in a second step. We will report about the status of the satellite design and the mission architecture.

INTRODUCTION

OHB Sweden has led two different phase A studies to assess the mission feasibility. Suitable satellite constellation configurations have been identified that may be considered to fulfil the objectives. Promising concepts that are considered for implementation are presented. For such small satellite concepts, low resource auroral imaging instruments are required. Such instrumentation is currently under development by ESA with the aim to enable multi-spectral imaging of the auroral emissions. Observation of multiple emission lines or band regions will enhance the reconstruction of the involved processes and allow thereby the characterization of the sources of the aurora and the identification of their location of origin. Additionally, as a goal, a small in-situ instrument suite including for example a magnetometer, hot plasma or electron analyzer and/or neutral atom mass spectrometer have been considered. The small satellite constellation will make progressively use of innovative and highly miniaturized space weather instrumentation, and be based on OHB's InnoSat: a robust, reliable, agile, and versatile small satellite platform [1].

Monitoring the Earth and Sun environment is an essential task for the nowcasting and forecasting of Space Weather (SWE) and the modelling of the interaction between the Sun and the Earth, as described in [2]. ESA is working towards the implementation of an Enhanced Space Weather Monitoring System that is making use of several observations carried out by sensors located on-board of several satellites and on ground. As part of ESA's Distributed Space Weather Sensor System (D3S –see [3]), which shall monitor the environment in the proximity of the Earth, the monitoring of the aurora is an essential and central nowcasting and forecasting element that enables direct observation of the impact of space weather events such as generated by strong solar wind variations and by Coronal Mass Ejections (CMEs). CMEs may cause geomagnetic storms and sub-storms when hitting the Earth. Auroral emissions (optical, far-UV and X-ray) are a direct manifestation of physical processes occurring

when the magnetosphere responds to the solar wind and CMEs when plasma streams and imprinted magnetic fields of CMEs strongly alter the interplanetary and geomagnetic field. The generated Auroral emissions contain information about the incident primary particles and about physical and chemical processes occurring locally.

The Aurora mission will observe emissions in the visible optical range and in the Far Ultra-Violet (FUV) spectral regions. Depending on the space weather conditions, the aurora has different local shapes and the Auroral Oval (AO) expands further towards the equator the stronger the space weather events are. For strong solar storms, the AO expands to low latitudes as far down as 40º or 50º North (e.g., to latitudes as low as Washington or Germany). The Aurora mission will be the first European operational mission to ensure 24/7 aurora observation data availability to support operational space weather applications. Auroral observations on both day and night sides of the Earth are essential for understanding the impact of the solar wind and CMEs. It complements existing ground based observations of magnetospheric substorms with reliable and global space based observations [4].

MISSION CONCEPTS

OHB has investigated several mission concepts and baselined a first mission concept in a 350x1500km flower constellation of six to eight satellites in a first Phase A study several years ago.

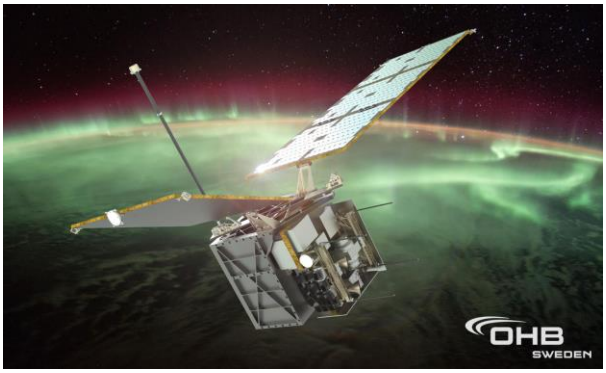

Figure 1: Satellite configuration as derived in the first mission study.

A second phase A study was then initiated more recently where an alternative and more promising mission concept was baselined: four satellites in a 6500km circular orbit, all in the same plane, separated by 90° in argument of perigee as depicted in Figure 3. This paper focused on this mission concept and elaborates on the orbit configuration and mission performance in terms of its observational capability and constraints.

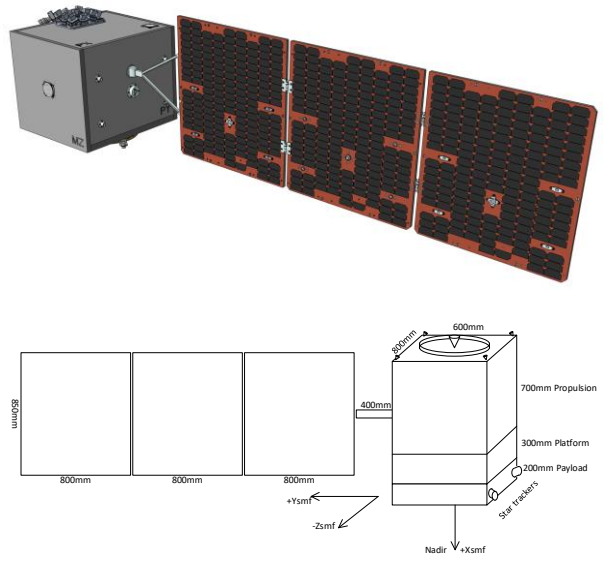

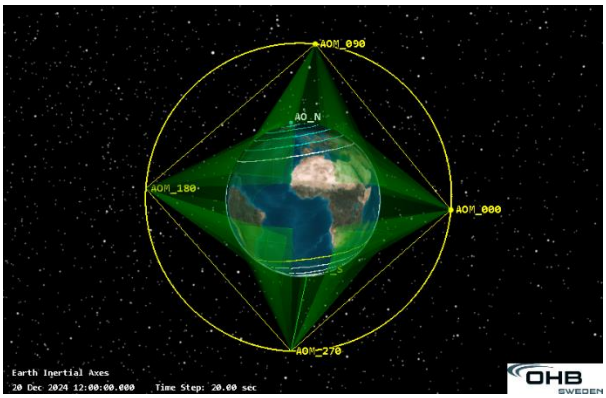

Figure 2: Visualization of the satellite configuration in the MEO orbit (altitude = 1 Earth radius) as baselined for the second study.

As shown in Table 1, several in-situ instruments considered in the first study were no longer baselined in the second study due to the different MEO environment since these instruments did not add as much value at this orbit compared to the lower elliptical orbits.

Table 1: Baseline payloads of the two studies.

Abbreviation	Instrument	6500 km circular	350 x 1500 km
AOSI	Auroral Optical Spectral Imager	X	X
AUI	Auroral UV Imager	X	X
RM	Radiation Monitor	X	X
MAG	Magnetometer	X	X
mNLP	Multi-Needle Langmuir Probe		X

INMS	Ion and Neutral Mass Spectrometer		X
HPA	Hot Plasma Analyser		X

OPERATIONS

Operations will be dominated by downlink, processing, and data dissemination using polar ground stations. Platform operations will be minimized to primarily health monitoring. ESA is planning to implement a demonstration mission (Aurora-D) to be launched in 2027 consisting of a single satellite in a first step and then to launch and operate a constellation (Aurora-C) in a next step planned for 2030. The current baseline configuration of the mission assumes a MEO orbit with altitudes between 6500 and 7000 km, which is also used in the considerations here below.

INTER-SATELLITE LINK

Aurora-C would benefit from an intersatellite link to ensure near-real time downlink of all satellite data. Aurora-D instead does not require this capability.

An Optical Inter-Satellite Link (OISL) may be used even as such a large inter-satellite distance. The communication distance for the 4-satellite equiangular constellation in a 6500km orbit is about 18212km to nearest neighbour. Laser based communication relieves concerns about ITU frequency sharing, encryption, and distance. Another advantage of OISL is that OTS units are often mounted on gimbals allowing for communication with both leading and following satellite neighbours after a 180° slew. No suitable alternative RF-based ISL has yet been identified due to the limitations described above. Satellite relay via geostationary satellites was also evaluated, but Aurora's high orbit altitude will lie outside of the earth-sized signal cones reducing communication coverage.

The impact of an ISL is quantified as the amount of time when data is collected before and after a passage over Svalsat, a Norwegian ground station in Svalbard. For data collection up to 50° from the AO center, ~50 minutes of data are stored before and after a passage, considering an average passage of ~78 minutes over the 4hr2min orbit period. Without an ISL, data collected outside of contact could be stored and forwarded with a corresponding latency of worst-case time between contacts, ~60 minutes.

The constellation communication concept assumes two neighbouring satellites to be in communication via ISL while one of them is in communication with a ground station. With Troll and Svalbard in opposing hemispheres, all four satellites in the 6500km circular orbit will be in constant communication with a ground station. In fact, the trigger to slew the ISL 180° and begin communication with the other satellite neighbour is performed when both satellites currently in ISL communication are simultaneously in range of the ground station.

ORBIT

The dedicated launcher or OTV provider is assumed to provide both orbit acquisition and phasing for each satellite. The platform propulsion system is sized only for orbit maintenance, collision avoidance, and transfer to graveyard. A European micro-launcher is currently baselined.

Beta Angle

The Beta Angle being defined as the angle between the satellite orbital plane and the geocentric position of the sun gives a quantitative value of the orbital shadowing that a satellite experiences, and important aspect to size its power and battery system and to judge the thermal constraints. The closer to an angle of 0°, the longer time fraction of its orbit the satellite will spend in Earth shadow. The drift in RAAN will be negligible for this orbit constellation, and therefore the Beta Angle profile over one year will be determined by the initial RAAN selected for the operational orbit (90°). The maximum and minimum Beta angles will vary between +/-66.6° as for RAAN 0° or RAAN 180° (see Figure 3), and +/-90.0° as for RAAN 90° or RAAN 270° (see Figure 4).

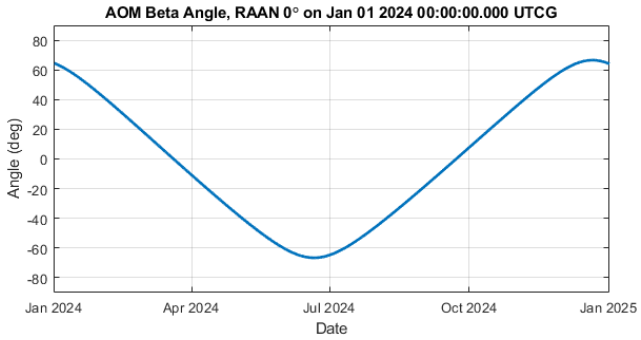

Figure 3: RAAN 0° gives Beta Angle between -66.6° and 66.6°, with a noon-midnight orbit around the vernal and autumnal equinoxes.

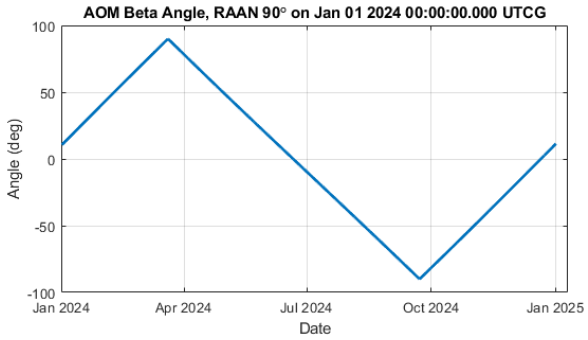

Figure 4: RAAN 90° gives Beta Angle between -90.0° and 90.0°, with a dusk-dawn orbit around the vernal and autumnal equinoxes.

Eclipses

Duration of eclipses and the eclipse periods were determined over one year for the RAAN 0° and RAAN 90° cases. Since the orbit is inertially fixed, there are two eclipse periods per year.

The maximum eclipse length with Earth as occulting body is 40.2 minutes. With an approximate orbit period of 242 minutes, this corresponds to 17% of one orbit duration in eclipse.

The eclipse periods do for the RAAN 0°/180° case occur around the equinoxes, while for the RAAN 90°/270° around midwinter and solstice, see **Error! Reference source not found.** and **Error! Reference source not found.**.

For the RAAN 0° case, eclipses for the simulated period, with the moon as occulting body, coincide with the eclipse periods, while for the RAAN 90° they are between the eclipse periods.

RAAN 90° case, the eclipse periods are slightly shorter for the RAAN 0° case, in the simulation 59.5 and 62.5 days versus 66.2 and 66.7 days.

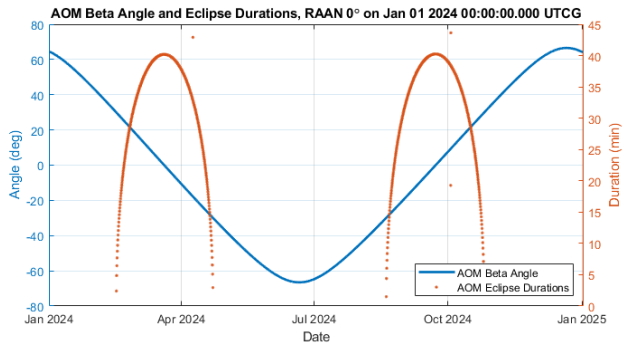

Figure 5: Eclipse Durations and Beta Angle with RAAN 0°.

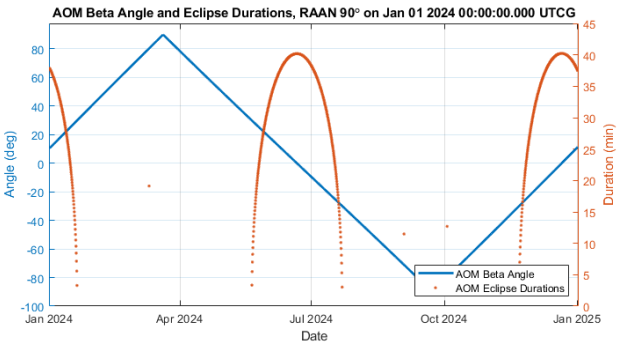

Figure 6: Eclipse Durations and Beta Angle with RAAN 90°.

SOLAR ARRAY DRIVE ASSEMBLY (SADA)

OHB Sweden's InnoSat platform is designed for LEO and typically flown in SSO. However, in MEO the LTAN will drift because the orbit is essentially inertially fixed.

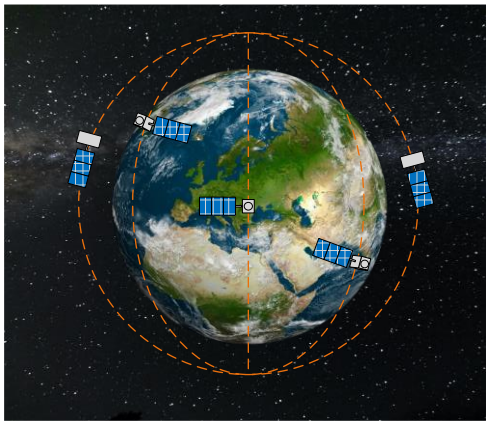

Figure 7: SADA and yaw guidance.

After trading off different Solar Array (S/A) configurations, a one-axis SADA has been chosen as the best compromise. A single S/A with SADA is placed perpendicular to the nominal nadir direction as shown in Figure 2. A yaw attitude can be chosen for each LTAN that is constant for the entire orbit to minimize the number of required yaw slews as shown in Table 2. The coordinate system, Spacecraft Mechanical Frame (SMF), is defined in Figure 2.

Table 2: Yaw guidance as function of LTAN.

LTAN	RAM direction	comment
03:00-09:00	-Ysmf	
09:00-12:00 and 21:00-24:00	-Zsmf	Avoids shading by body on S/A
12:00-15:00 and 24:00-03:00	+Zsmf	As above
15:00-21:00	-Ysmf	

The resulting cosine losses of the above SADA and yaw guidance strategy are plotted below by season and LTAN.

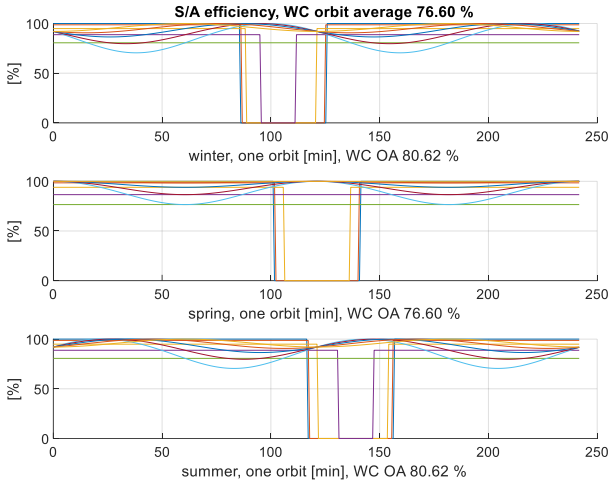

Figure 8: S/A efficiency as function of season and LTAN.

RADIATION ANALYSIS

The environment definition is carried out with Spenvis. The classic AE8 max/AP8 min model is used to determine trapped particles and the SHIELDOSE-2 model to calculate the Total Integrated Dose (TID) levels. Several different orbits were compared. The following set of elliptical orbits which are sun-synchronous and critically inclined at the same time was found to present the same radiation environment both in terms of proton flux and TID. For this reason, only one of them was arbitrarily chosen to represent this set of orbits:

- 600 x 7685 km
- 700 x 7470 km
- 800 x 7260 km
- 900 x 7050 km
- 1000 x 6850 km
- 1100 x 6660 km

The next set of orbits analysed are circular polar orbits in MEO with the following altitudes:

- 6000 km
- 6371 km
- 6500 km
- 7000 km
- 7500 km

Finally, for comparison, a critically inclined 350 x 2500 km orbit was also analysed.

In summary, without presenting the details of the analysis, it was shown by the analyses that the elliptical orbits are very harsh in terms of proton flux and TID while circular orbits have lower proton flux that decreases as the altitude gets higher.

In a similar manner, also for the TID , the elliptical orbits present a challenging radiation environment while for the circular orbits above 6000 km the TID level starts to become acceptable and further decreases as the altitude increases.

SENSOR COVERAGE

This section presents figures of merits related to the nadir pointing sensor (imager) coverage of the Auroral Oval, which is considered as a major performance figure of the mission.

The centre of Northern Auroral Oval (NAO), corresponding to the predicted northern geo-magnetic pole 2025, is defined in spherical coordinates as:

- Latitude: 80.9°
- Longitude: -72.6°

The area analysed for coverage is defined as:

- Distance Radius: 6488.14 km (Earth Equatorial Radius + 110 km)
- Area Radius:
    - 3000.0 km
    - 4529.57 km (corresponding to 50° geo-magnetic latitude)
    - 5095.77 km (corresponding to 45° geo-magnetic latitude)
- Grid Granularity: 1° (Lat/Long)

The centre of Southern Auroral Oval (SAO), corresponding to the predicted southern geo-magnetic pole 2025, is defined in spherical coordinates as:

- Latitude: 80.9°
- Longitude: 107.4°

The area analysed for coverage is defined as:

- Distance Radius: 6488.14 km (Earth Equatorial Radius + 110 km)
- Area Radius:
    - 3000.0 km

- 4529.57 km (corresponding to 50° geo-magnetic latitude)
- 5095.77 km (corresponding to 45° geo-magnetic latitude)

- Grid Granularity: 1° (Lat/Long)

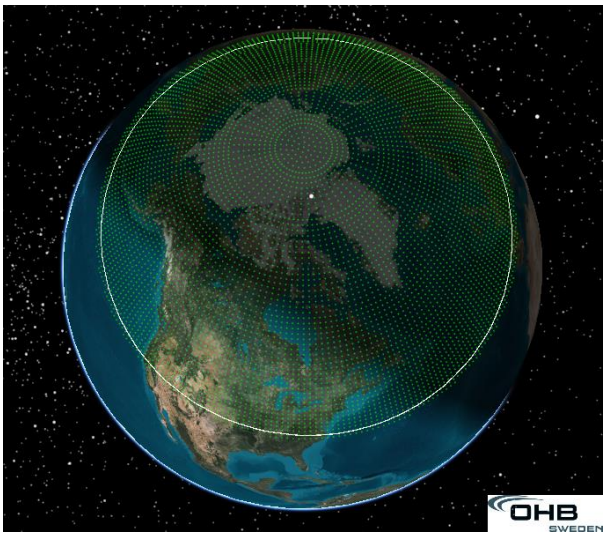

Figure 9: Northern Auroral Oval area with grid points to 45° geo-magnetic latitude.

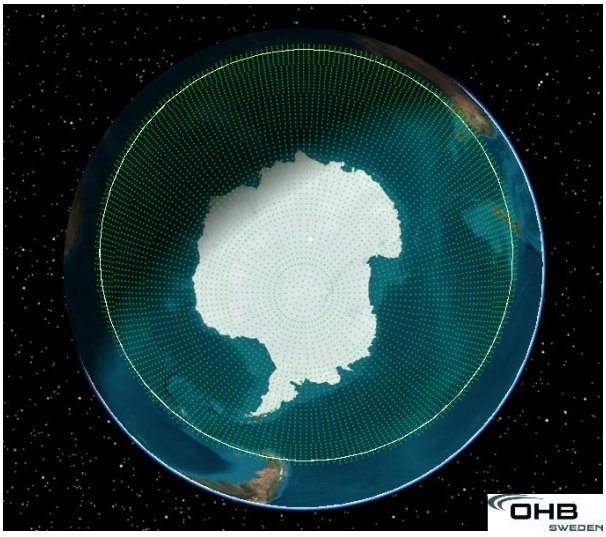

Figure 10: Southern Auroral Oval area with grid points to 45° geo-magnetic latitude.

Simple Coverage

We define Simple Coverage as a measure of whether a point of the AO is accessible by the imagers or not. An evaluation of the dynamic behaviour of this coverage computes a value of 1 for points that are currently in an access period and 0 for points that are not. The static behaviour of Simple Coverage computes a value of 1 for grid points that have access to an asset at any point in time and 0 for points that are not accessible. Plots of Current Area Coverage and Accumulated Area Coverage, both in percent of the target area (NAO or SAO), are also presented. Current area coverage is the percentage of the target area covered by the sensors at a certain instant of time. Accumulated area coverage is the percentage of the target area covered from the start of the simulation up to a certain instant of time. Time to reach maximum accumulated area coverage is measured with start from the instant of time with minimum current coverage.

Table 3: Summary of the NAO Area Coverage.

AO Range From Geo-magnetic Centre	Total Accumulated SAO Area Coverage (%)	Current SAO Area Coverage	AO Range From Geo-magnetic Centre	Total Accumulated SAO Area Coverage (%)
		Minimum	Maximum	Average
3000 km	100.0	93.7	100.0	97.6
40°	100.0	91.4	100.0	95.3
45°	100.0	88.6	97.9	92.6

We note that these results as summarised in Table 3 and 4 represent an excellent performance meaning that the AO is visible almost continuously, which is one of the primary mission goals.

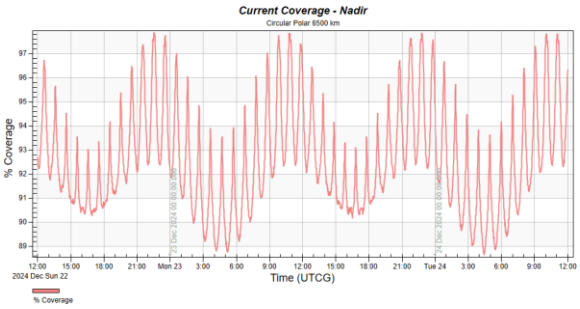

Figure 11: NAO Current Coverage Plot.

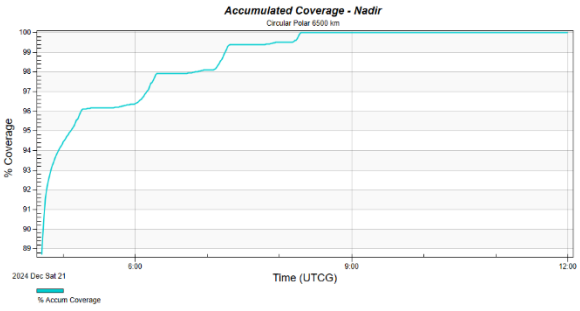

Figure 12: NAO Accumulated Coverage Plot.

This orbit configuration will ensure at least 91.9% instantaneous coverage of the imagers at any time (Figure 115), with 100% accumulated coverage of the NAO 45° within at most 3 hr 36 min (Figure 126).

Table 4: SAO Area Coverage

AO Range From Geo-magnetic Centre	Total Accumulated SAO Area Coverage (%)	Current SAO Area Coverage	AO Range From Geo-magnetic Centre	Total Accumulated SAO Area Coverage (%)
		Minimum	Maximum	Average
3000 km	100.0	93.7	100.0	97.6
40°	100.0	91.5	100.0	95.3
45°	100.0	88.7	97.9	92.6

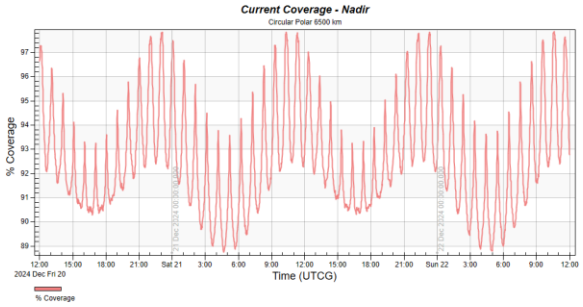

Figure 13: SAO Current Coverage Plot.

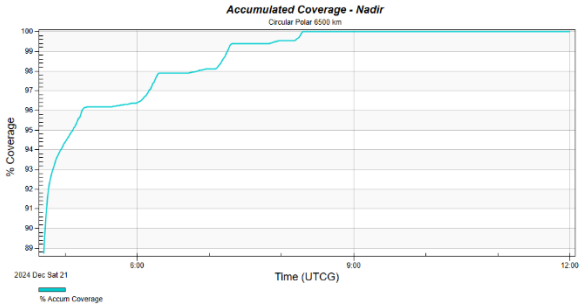

Figure 14: SAO Accumulated Coverage Plot.

We also conclude that the MEO orbit will ensure at least 61% instantaneous coverage of the imagers at any time (Figure 13) with 100% accumulated coverage of the SAO within at most 3 hrs 36 min (Figure 148).

Coverage Time in Percent

The coverage time does initially radially increase from the north pole to latitude 63° to then decrease as shown in Figure 159. Note that the "Minimum", "Maximum" and "Average" curves relates to the statistics of the grid points at each latitude.

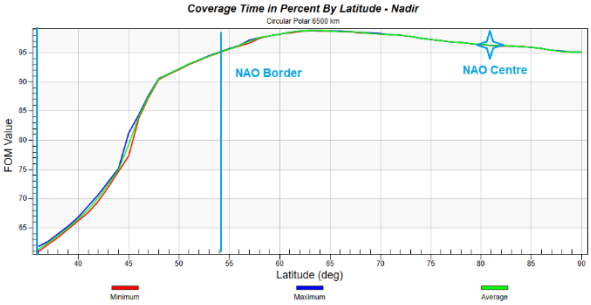

Figure 15: NAO Coverage Time in Percent by Latitude

Just within 30° from the NAO centre, the coverage time is always above 94%. The coverage time quickly decreases down to approximately 61% at 45° from the NAO centre, farthest from the north pole, with the opposite side at being close to 100%.

Table 5: NAO Coverage Time Statistics.

AO Range From Geo-magnetic Centre	NAO Coverage Time (%)		
	Minimum	Maximum	Average
3000 km	95.1	98.8	97.5
40°	68.8	98.8	95.3
45°	60.9	98.8	92.6

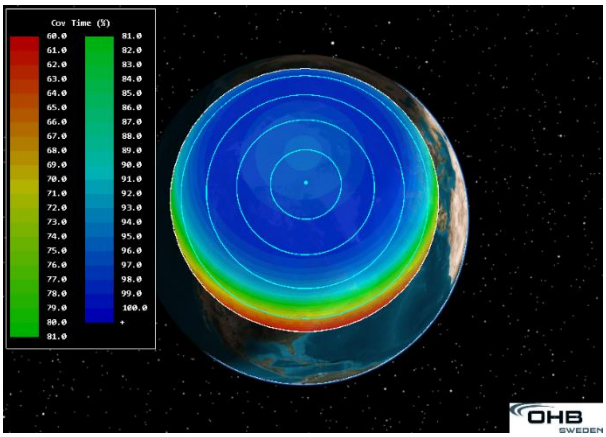

Figure 16: Map of Coverage Time in Percent.

The time does initially radially increase from the south pole to latitude -62° to then decrease quickly. Between SAO centre and -30° the coverage time is always above 90%, but outward then quickly decreasing down to approximately 61% at 45° from the SAO centre at the point farthest from the south pole, with the opposite side being close to 95%.

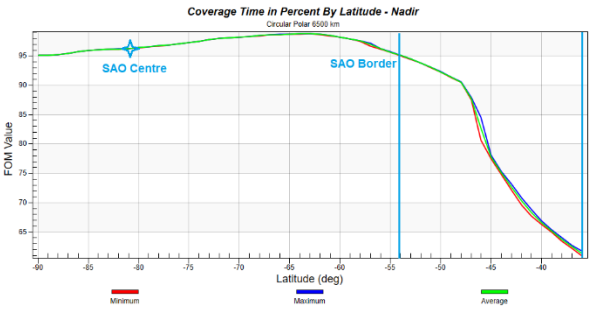

Figure 17: SAO Coverage Time in Percent by Latitude

Table 6: SAO Coverage Time Statistics

AO Range From Geo-magnetic Centre	SAO Coverage Time (%)		
	Minimum	Maximum	Average
40°	68.9	98.8	95.3
45°	60.9	98.8	92.6

GLOBAL PERFORMANCE

The map of the coverage time (in percent) of the globe includes the NAO and SAO, Figure 18 to Figure 20, and is here complemented by the plot in Figure 21 showing global coverage time in percent by latitude. The reduced coverage time above the poles (+/-90°) compared to the coverage at e.g. latitude 50° is due to the fact that the areas covered by the sensors of two adjacent satellites do not fully overlap when the mid-point of their orbit positions passes above the poles, an effect of the earth ellipsoid.

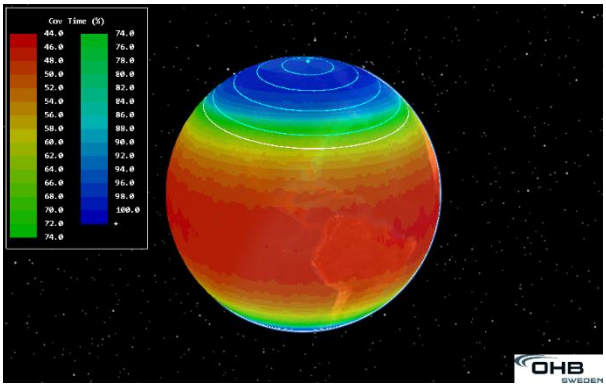

Figure 18: Global Coverage Time in Percent.

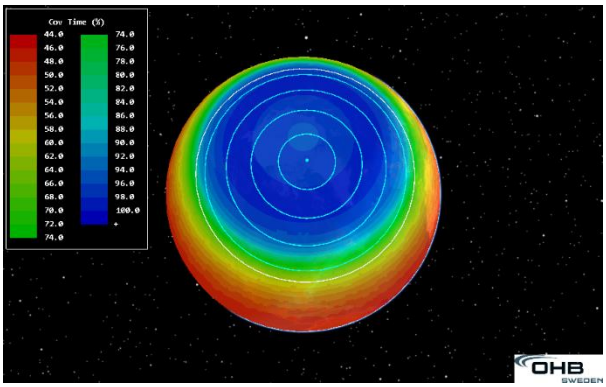

Figure 19: Global Coverage Time in Percent around the northern geo-magnetic pole

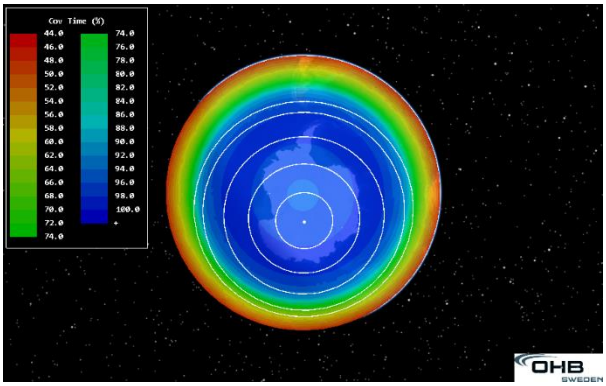

Figure 20: Global Coverage Time in Percent around southern geo-magnetic pole.

Table 7: Global Coverage Time Statistics.

Global Coverage Time (%)		
Minimum	Maximum	Average
45.5	98.8	65.9

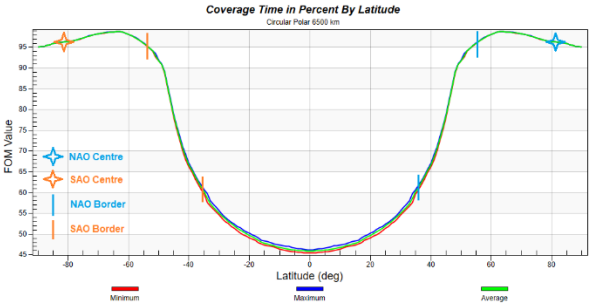

Figure 21: Plot of Coverage Time in Percent by Latitude used as figure of merit.

Data Latency

The latency, here defined as the time from the collection of data until it is possible to downlink the data, was estimated using Ansys STK and MATLAB by analysing the times of coverage at different distance from centre and of coverage of the satellites from the ground stations over four (4) days: 20 Dec 2024 12:00:00.000 UTCG to 24 Dec 2024 12:00:00.000 UTCG, see Figure 22 for a selected period.

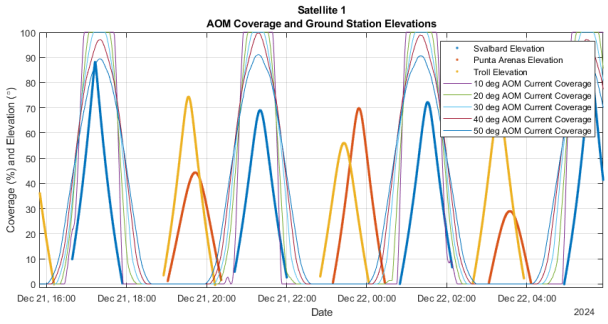

Figure 22: Coverage and Ground Station Coverage.

The maximum latency, not including level 1 processing, is determined for the data collected before start of nearest pass for SvalSat (same as the data collection duration prior to pass) and for data collected after the pass until next pass over SvalSat (same as the time from end of pass until start of next pass) for a single satellite, see Figure 23. SvalSat is KSAT's Svalbard Satellite Station. For the constellation, Aurora-C, the intention is to complement SvalSat with KSAT's TrollSat Satellite Station in Antarctica to support observation of the SAO.

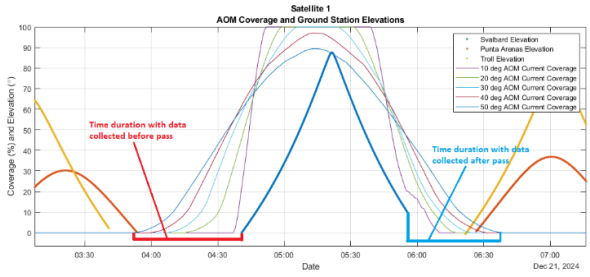

Figure 23: Time duration of data collection before and after pass.

The period of data collected immediately before the pass is estimated from 50°, 40°, 30° and 20° degrees from the AO centre and is in this analysis called "pre-latency". As example for Satellite 1 and SvalSat, the maximum latency for data collected 50° from AO centre until earliest possible download is approximately 49.2 minutes, and when considering all satellites, 50.4 minutes.

The period of data collected immediately after a pass is also estimated for the different distances from AO centre, which in this case corresponds to the position when the data ceases to be collected. The maximum data latency for this data until earliest possible download in next pass – in this analysis called "post-latency" - is therefore independent of the stop collection distance from AO centre, but rather depends on the time from the end of pass to the start of next pass. As example for Satellite 3 and SvalSat, data collected up to 50° from AO centre for a maximum duration of 49.3 minutes may be delayed for a maximum time of 168.4 minutes before being earliest available for download.

Table 8: Data Collection Durations and Latencies computed for the SvalSat Ground Station.

Satellite	AO Start/Stop Collection Distance (°)	Max Duration (min)		
		Data Collection Before Pass N (Pre-Latency)	Data Collection After Pass N	Data Latency After Pass N until Pass N+1 (Post-Latency)
1	50	49.2	49.6	169.4
	40	41.8	42.3	
	30	34.2	34.6	
	20	24.8	26.3	
2	50	50	49.6	168.7
	40	42.8	42.2	
	30	34.8	34.6	
	20	25.8	25.2	
3	50	50.4	48.1	168.5
	40	43.1	41.1	
	30	34.7	34.1	
	20	26.1	26.3	
4	50	49.7	49.3	168.4
	40	42.7	42.3	
	30	34.7	34.3	
	20	25.3	26.4	
Total	50	50.4	49.6	169.4
	40	43.1	42.3	
	30	34.8	34.6	
	20	26.1	26.4	

With an ISL, the latency will drastically improve the real-time availability of the data, considering that fixed pointing observations are made simultaneously with ground station communications. With bi-directional ISL, up to 100% real-time availability may be reached in such a scenario: "pre-latency" data can be made available in real-time via the satellite forward in track, and "post-latency" data via the satellite tracking behind.

If unidirectional ISL is to be used, the recommended ISL data flow direction is toward the satellite tracking behind giving larger reduction in total data latency, than having

the data flow toward the forward tracking satellite. Note that only one ISL connection per satellite is required, since a maximum of two sensors may simultaneously cover any portion of NAO area down to latitude 45°.

SUMMARY AND CONCLUSIONS

A satellite and constellation concept has been developed to meet the mission needs of continuous auroral observations which is based on the utilization of the InnoSat small satellite platform. By careful choice of orbit, the mission observation needs can be met with an adapted platform originally designed for LEO. The first Aurora-D single satellite mission being implemented shall demonstrate the mission concept and pave the way towards a follow-on four satellite constellation (Aurora-C), which shall then become operational as part of ESA's future enhanced space weather monitoring system.

References

1. B. Lagaune et al., Arctic Weather Satellite, A microsatellite constellation for improved weather forecasting in Arctic and globally, 35th Annual Small Satellite Conference, SSC21-XII-02
2. S. Kraft et al., Aurora: A Small Satellite Constellation for Auroral Oval Monitoring, 73rd International Astronautical Congress (IAC), Paris, France, 18-22 September 2022. Copyright 2022 by ESOC - European Space Agency. Published by the IAF, with permission and released to the IAF to publish in all forms. IAC-22.B4.IP.x35329
3. ESA's distributed space weather sensor system (D3S) utilizing hosted payloads for operational space weather monitoring, Acta Astronautica Volume 156, March 2019, Pages 157-161, https://doi.org/10.1016/j.actaastro.2018.01.020
4. K. Kauristie et al., Ground-based and satellite observations of high-latitude auroral activity in the dusk sector of the auroral oval, Annales Geophysicae (2001) 19: 1683–1696